International Journal of Engineering Science, Advanced Computing and Bio-Technology
Vol. 5, No. 3, July – September 2014, pp. 76 -86

# The Effectof Modeof Additionand Agitation on the Morphology of NanoHAp in Coprecipitation Method

P.Michael SL Shanthi[1], M.Ashok[1], R.V.Mangalaraja[2] and T.Balasubramanian[1]

[1]*Nano materials Lab, Department of Physics, National Institute of Technology, Tiruchirrappalli-620 015, TamilNadu, India.*

E-mail: *ashokm@nitt.edu*

[2]*Department of Materials Engineering, University of Concepcion, Concepcion, Chile, Latin America*

***Abstract:*** *The preparation of Nano hydroxyapatite (HAp) with varied morphology has usually been achieved by changing the parameters like concentration, temperature, pH and the precursors in coprecipitation method. However the morphological control by changing the mode of addition of the precursor solutions has seldom been reported. In the present work polygonal morphology has successfully been achieved by a simple method of dripping the calcium ionic solution through a tubular tip into the whirl-pool of tetradecyltrimethylammonium bromide (Cetrimide) added phosphate ionicsolution, which is stirring moderately. The same experiment with ultrasonic vibration instead of stirring has also been done. The Fourier Transform–Infrared Spectroscopy (FTIR), X-ray diffraction (XRD), Scanning Electron Microscope (SEM), Energy dispersive X-ray spectroscopy(EDX) and Transmission Electron Microscope (TEM) studies were made and the results were discussed. The results show that polygonal morphology could be achieved by changing the mode of addition. The change in mode of agitation gives comparatively smaller particles with smaller grain size, more strain and carbonate inclusion.*

***Keywords:*** *hydroxyapatite; surfactant; coprecipitation method; polygonal; morphology.*

## 1. Introduction

Hydroxyapatite is a type of calcium phosphate with excellent biocompatibility and osteointegrity and hence it is a well-known material in the field of dentistry and orthopaedics. The Modern technological advancements expand the scope of application of HAp beyond its conventional applications like space filling, artificial bone graft, maxillofacial, biocompatible coating etc. For example, Nanotechnology extends its usage in the field of novel drug delivery and tissue engineering. However the size and morphology confinement of HAp, which decides the choice of application, is a big challenge in nanotechnology. Hence various methods of preparation have been adopted to overcome this problem.

Received: 26 June, 2014; Revised: 07 August, 2014; Accepted: 22 September, 2014

Biomimetic, Solid-state synthesis, mechanochemical, hydrothermal, chemical precipitation and coprecipitation are the various methods used to synthesize the nanoHAp. Among them coprecipitation method is a recent one which establishes good control over the morphology and size of the particles. Literature reports that co precipitating agents play a vital role in the preparation of nano particles rather than the simple precipitation method. Plazzo et al has reported that the polar amino acids induce a morphological and dimensional variation in calcium-deficient hydroxyapatite (CDHA) nano crystals rather than the CDHA prepared without the amino acids [1].Martínez-Pérez et al. reported that the 2% and 5% addition of β-cyclodextrin (β-CD) as a coprecipitating agent controls the size to nano and also reduces the impurity inclusion [2]. The surfactants like CTAB, SDS, EDTA, PEG, pluronic-127, etc. have also been used to prepare nanoHAp. In such works the concentration plays an important role in modifying their morphology and size from rods to spheres and even to plate-like HAp particles [3-10].Morphological modification has also been achieved by optimizing the other parameters like temperature and pH. The work based on pH variation reports that the higher hydrogen ion activity due to high pH results in spherical Hap, whereas low pH in rods and whiskers [11]. Similarly HApprepared with high temperature results in the growth of the particles size[12].

A trend of engineering the particles by incorporating simple modifications in the existing methods has also been emerging. In coprecipitation method, Zhang et al. has reported the preparation of poly dispersed spherical HApparticles by simply changing the rate of addition of the precursors [13].Cai et al. has reported the CTAB assisted hollow spherical HAp particles by changing the mode of mixing [14]. In the same way, the present work reports the control over the morphology by changing the way of addition of precursors, which was not reported earlier. In our previous report by using the cationic surfactant 'Cetrimide' of 4mM, we have achieved hollow spheres of Hap [15].Current work reveals that, a simple change in mode of addition of the same method could tailor the morphology from hollow spheres to polygonal. Similarly the change in the mode of agitation or mixing, i.e. using ultrasonic vibration instead of stirring, resulted in disintegration of particles to smaller size.

## 2.1 Materials

The precursors diammoniumhydrogenphosphate $(NH_4)_2HPO_4$ and calciumnitratetetrahydrate $Ca(NO_3)_24H_2O$ were purchased from Merck Specialties Private Limited, India. Sodium hydroxide pellets (NaOH) were bought from Qualigens Fine Chemicals, India. The capping agent Cetrimide ($C_{17}H_{38}NBr$) was purchased from Merck, India.

## 2.2 Experimental procedure

The aqueous solution of $(NH_4)_2HPO_4$ (0.6 M) was added with 4 mM of cetrimide and stirred well. The pH was raised to ~11.5 using 1M of NaOH. The aqueous solution of $Ca(NO_3)_2.4H_2O$ (1M) was dripped slowly through a tube by dipping it into the whirl-pool of stirring $PO_4^{3-}$ solution. White milky solution was obtained;from which white sample was filtered, dried and named as HAp-D. The experiment was done at ambient temperature. The same experiment was repeated with normal way of addition while the mode of agitation has been changed. The ultra-sonic vibration of frequency 40 kHz and energy 150 W was used for mixing instead of stirring. The variation in temperature was maintained between 50 to 53°C. The white precipitate obtained was dried and named as HAp-S. Both the precipitates were calcinated at 750°C for 8 h and named as HAp-D750 and HAp-S750.

**Characterization**

The samples were subjected to different characterizations. The chemical bonding structures of the samples were confirmed by the Fourier Transform–Infrared Spectroscopy (Perkin Elmer Spectrum RX1). The structural and phase analysis were done by the X-ray diffraction technique, using RigakuUltima III with Cu Kα (1.54056 Å)radiation. The structure and chemical composition of the samples were examined by a JEOL JSM 6380 LV Scanning Electron Microscope with the attachment of Energy dispersive X-ray spectroscopy.The morphologic analyseshave been carried out using a JEOL JEM 1200 EX II Transmission Electron Microscope.

## 3. Results and Discussion

**3.1FTIR analysis**

The FTIR spectrum of as precipitated HAp-S sample is given in Fig.1(a) and that of calcinated HAp-S-750 and HAp-D-750 samples are given in Fig.1(b) and 1(c) respectively.

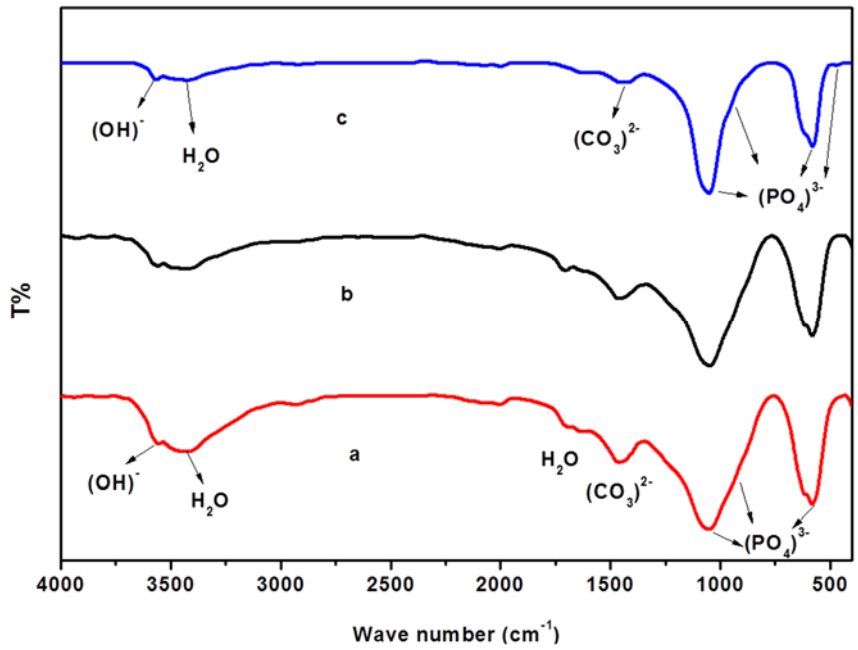


**Fig.1. FTIR spectra of: (a) HAp-S, (b) HAp-S750 and (c) HAp-D750 samples.**

The FTIR spectra show all the stretching and bending vibrations of the phosphate mode and the OH functional group. The broad and strong peak between1000-1100 $cm^{-1}$ belongs to the stretching mode of phosphate functional group. Similarly the strong peaks in between 500 to 600 $cm^{-1}$ are due to the bending mode of the phosphate group. The sharp peaks at 3566 $cm^{-1}$ of HAp-D750 sample and that around 3560$cm^{-1}$ of HAp-S and HAp-S750 samples belong to the stretching vibrations of the OH functional group. They confirm the presence of HAp, as they are considered to be the characteristic peaks of Hap [16, 17]. The broad peak around 3430 $cm^{-1}$ of HAp-S sample (Fig.1 (a)) is from the lattices of water molecules and henceit becomes smaller (Fig.1 (b) &1(c)) after thermal treatment. The carbonate ion insertion is observed at 1461 $cm^{-1}$ andwhichdenotes the 'B' type substitution of few $PO_4^{3-}$ ions by $CO_3^{2-}$ ions [18]. The inclusion of these carbonate ionsare mainly from the organic template material. Sincethe presence of template material inthe as prepared HAp-S sample is also detected from the weak peak at 2935 $cm^{-1}$ that belongs to the stretching vibration of C-H group. However the removal of template material is also confirmed from the absence of the same in the calcinated samples HAp-S750 and HAp-D750.

### 3.2 XRD analysis

The XRD patterns of calcinated HAp-D750 and HAp-S750 samples are given in Fig. 2(a) and 2(b) respectively. The peak positions and intensities of the samples are in good agreement with the JCPDS reference data 09-0432 which is given in Fig.2(c). The XRD

analysis confirms the hexagonal phase of the samples with space group $P6_3/m$ and no other impurity peak is observed. The XRDA software was used to calculate precise lattice parameters and the extracted data are given in Table 1. The crystalline phase fraction of the samples were calculated (Table.1) from the formula[19],

$$X_c = 1 - \frac{V_{112/300}}{I_{300}} \quad (1)$$

Where, $V_{112/300}$ is the intensity of the hollow between (112) and (300) diffraction peaks and $I_{300}$ is the intensity of (300) diffraction peak. Both the samples show a shrinkage in lattice parameter values (Table.1), as an indication of 'B' type substitution [20].

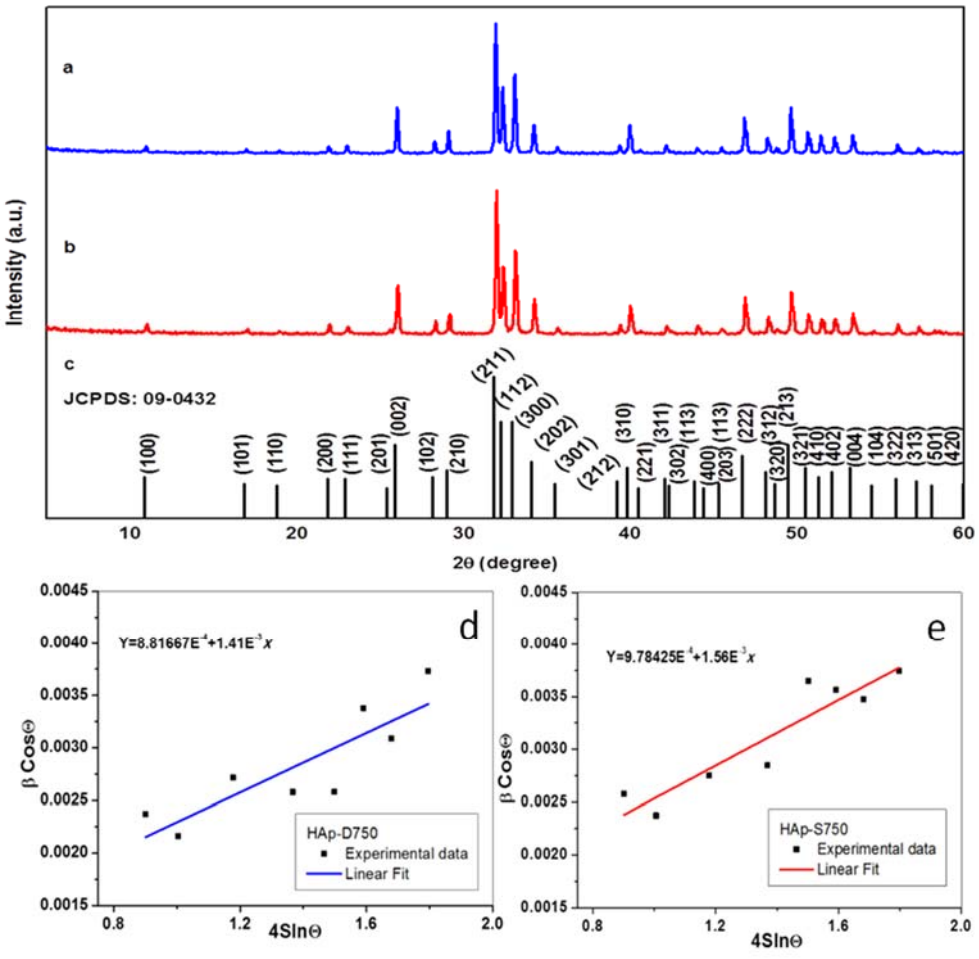


**Fig.2. XRD pattern of calcinated: a) HAp-D750, b) HAp-S750 samples and c) JCPDS: 09-0432.: (d) & (e) The plot between $4\sin\theta_{hkl}$ and $\beta_{hkl}\cos\theta_{hkl}$ of sample HAP-D750 and HAp-S750 respectively.**

The tetrahedral phosphate ions were replaced by the smaller planar carbonate ions in 'B' type substitution and hence the shrinkage [3]. The FTIR pattern also reflected the same result.

The conventional Williamson-Hall (W-H) method is an appropriate approach for the estimation of lattice strain. It assumes that the strain present in the material is uniform.Using the W-H method the average crystallite size and strain of the samples were obtained from the intercept and slope of the graph plotted between $4\sin\theta_{hkl}$and $\beta_{hkl}\cos\theta_{hkl}$values ofthe samples [21,22]. Here, $\theta$ is the Bragg's angle of diffraction, $\beta_{hkl}$ is the instrumental error corrected full width at half maximum of the diffraction peak (fwhm) in radian and $\varepsilon$ is the strain. The W-H plot of the samples HAp-D-750 and HAp-S-750 are given in Fig. 2(d) and 2(e) respectively and the values calculated are given in Table1.

| Sample name | Cry. Phase % ($X_c$%) | Lattice parameters (Å) | | | Unit volume (Å)$^3$ | Ave. grain size (nm) | Strain ($\varepsilon$) $\times10^{-3}$ |
|---|---|---|---|---|---|---|---|
| | | a | c | c/a | | | |
| HAp-D750 | 95% | 9.376 | 6.863 | 0.732 | 522.5 | 157.3 | 1.41 |
| HAp-S750 | 93% | 9.365 | 6.859 | 0.732 | 520.9 | 141.7 | 1.56 |
| JCPDS:09-0432 | - | 9.418 | 6.884 | 0.731 | 528.8 | - | - |

**Table 1.Geometrical parameters of the samples calculated from the XRD data**

The better fit of the experimental data points confirms the uniformity of the lattice strain. The points of HAp-S-750 are close to linear fit and hence the strain is uniformly distributed rather than the other sample.The average crystallite size of HAp-S-750 sample is lower than the HAp-D-750 and which is in agreement with the TEM images.

### 3.3. Electron microscopic analysis

The SEM images of HAp-D750 and HAp-S750 samples are given in Fig.3 (a) and Fig.3 (b) respectively. The SEM images reveal the nano size of the prepared samples.

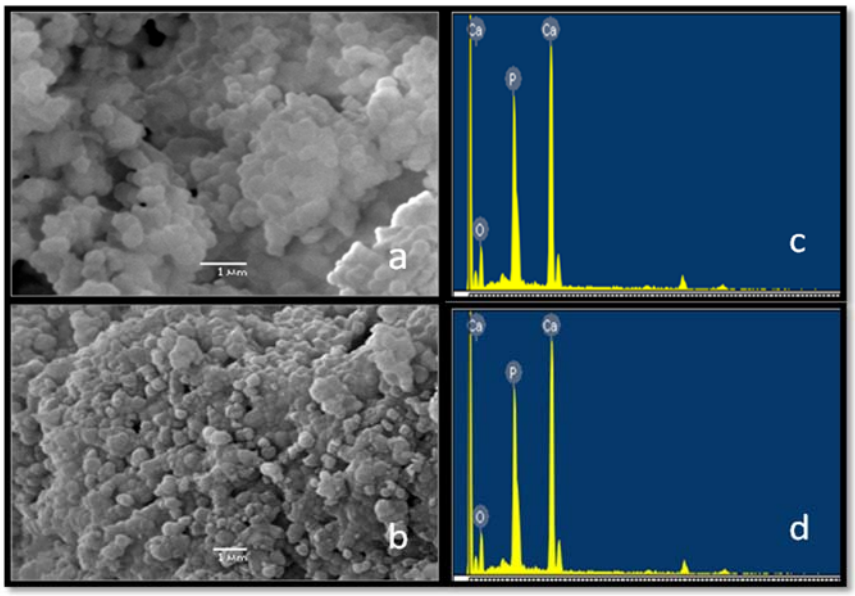


**Fig.3. SEM images of: (a) HAp-D750 and (b) HAp-S750 samples; EDX spectra of: (c) HAp-D750 and (d) HAp-S750 samples.**

The HAp-S750 sample is more spherical than the HAp-D750 sample and howeverthe study of morphology needs TEM analysis.The energy dispersive X-rayspectra of HAp-D750 and HAp-S750 samples are given in Fig.3 (c) and 3 (d) respectively. Thestoichiometric ratio (Ca/P) of the samples obtained from the EDX spectrum is given in Table 2.

| Sample name | Ca/P ratio | *x* value | The precise formula |
|---|---|---|---|
| HAp-D750 | 1.65 | 0.1212 | $Ca_{9.9394}(PO_4)_{5.8788}(CO_3)_{0.1212}(OH)_2$ |
| HAp-S750 | 1.61 | 0.3063 | $Ca_{9.8469}(PO_4)_{5.6973}(CO_3)_{0.3063}(OH)_2$ |

**Table 2. The stoichiometric ratio of the samples obtained from the EDX spectrum and the precise formulae of the samples.**

The Ca/P ratio (1.65) of the HAp-D750 sample(Fig.3 (c)) is close to the theoretical value 1.67 of the standard HAp. The low Ca/P ratio (1.61) of HAp-S750 sample (Fig.3 (d)) shows the inclusion of carbonate ions or the incomplete reaction. This implies that the ultrasonic vibration enhances the carbon inclusion rather than the desired internal ($Ca^{2+}$+ $PO_4^{3-}$) reaction.

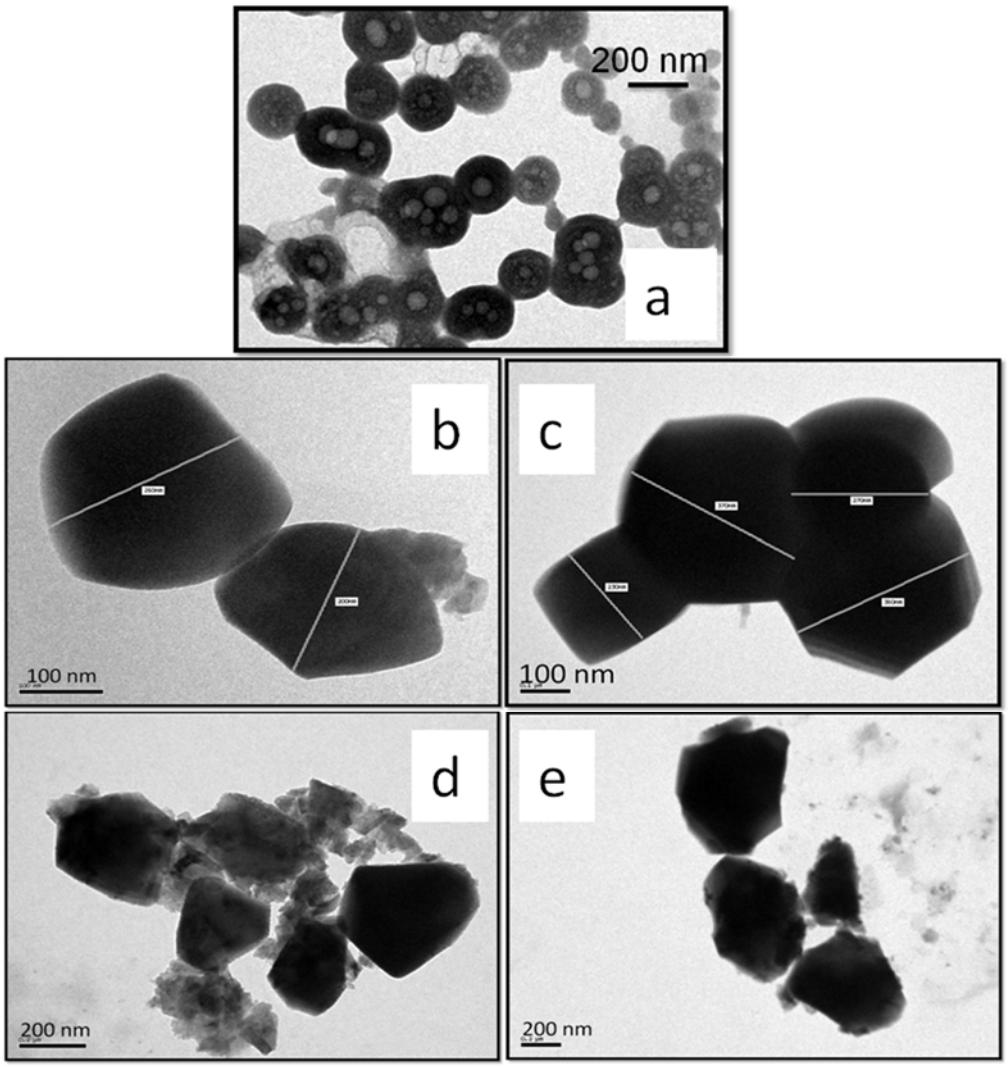


**Fig.4. TEM images of: (a) HAp- reference sample, (b) & (c) HAP-D750 sample, and (d) & (e) HAp-S750 sample.**

The carbonate content of the HAp can be calculated from the Ca/P ratio, by substituting the value of *x* in the chemical equation '$Ca_{10-x/2}\ (PO_4)_{6-x}\ (CO_3)_x\ (OH)_2$', where '*x*' is given by the formula [23],

$$x = \frac{(10 - (6 \times Ca/P))}{0.5 - (Ca/P)} \tag{2}$$

Thus the *x* values calculated and the corresponding formulae deduced for the samples HAp-D750 and HAp-S750 are given in Table 2.

The TEM images of HAP-D750sample are given in Fig.4 (b)&Fig.4(c) and that of HAp-S750 are given in Fig.4 (d)&Fig.4 (e). As a comparative measure the TEM image of the HAp particles prepared with the same experimental parameters, using normal mode of addition and agitation has been given in Fig.4 (a) [15].The TEM images reveal the transformation of the hollow sphere like morphology into polygonal structures. The open pores found in Fig.4 (a) could not be seen in the sample HAp-D-750 (Fig.4 (b) &4(c)), which implies that the closed micelle formation process has been accelerated. At the same time the face of the micelle which comes in contact with the tube becomes flat and consequently the HAp nucleates over these edged micelles and produces polygonal particles. The spinning fluid maintains this contact due to continuous stirring and thus the process continues.Similarly in the other method, the ultrasonic vibration enhances the dynamics of monomers in the micelles and acts against stabilization. This in turn causes indefinite morphology and size of particles. This result contradicts with the earlier report of Cai et. al, in whichhollow spheres have been obtained with the use of CTAB and ultra-sonication [14].

## 4. Conclusion

The flexibility of the surfactant assisted coprecipitation method has been studied by applying simple modifications to the conventional method of preparationof HAp. The experiment was conducted at room temperature using the surfactant 'Cetrimide'of 4 mM as template material with the pH 11.5. The same experimental parameters with normal mode of addition could result in hollow spheres of nano HAp as we reported earlier. However the current work reveals the fact that the immersed mode of addition, the neglected parameter, could tailor the morphology of nano HAp to polygonal. We hope further study over the rate of stirring along with the change in the size of the dripping tubes could result in more precise morphology control. Similarly, applying theultrasonic vibrationsinstead of stirring,in the second experiment resulted in the disintegration of the particles at the cost of morphology.

## References:

[1] Palazzo B, Walsh D, Iafisco M, Foresti E, Bertinetti L, Martra G, et al. Amino acid synergetic effect on structure, morphology and surface properties ofbiomimetic apatite nanocrystals. Acta Biomater 2009;5:1241–52

[2] Carlos A. Martínez-Péreza, Jorge García-Montelongoa, Perla E. Garcia Casillas, José R. Farias-Mancillaa, Humberto Monreal Romerob, Preparation of hydroxyapatite nanoparticles facilitated by the presence of β-cyclodextrin, Journal of Alloys and Compounds 536S (2012) S432– S436.

[3] Lin K, Chang J, Cheng R, Ruan M. Hydrothermal microemulsion synthesis of stoichiometric single crystal hydroxyapatite nanorods with mono-dispersion and narrow-size distribution. Mater. Lett. 2007;61:1683-87.

[4] Shanthi PMSL, Ashok M, Balasubramanian T, Riyasdeen A, Akbarsha MA. Synthesis and characterization of nano-hydroxyapatite at ambient temperature using cationic surfactant. Mater. Lett 2009;63:2123- 25

[5] Liu C, Xiujie Ji, Cheng G.Template synthesis and characterization of highly ordered lamellar hydroxyapatite .*Appl. Surf. Sci.* 2007; 253:6840–43.

[6] Shanthi PMSL, Ashok M, Mangalaraja RV, Balasubramanian T. Synthesis and Characterization of Nano Crystalline Hydroxyapatite spheroids using anionic Template for Bio Applications. Key Engineering Materials2012; 493-494:723-27

[7] Zhu R, Yu R, Yao J, WangD, Ke J. Morphology control of hydroxyapatite through hydrothermal process. J.Alloy. Compd2008;457:555-59

[8] Qiu C, Xiao X, Liu R. Biomimetic synthesis of spherical nano-hydroxyapatite in the presence of polyethyleneglycol. Ceram.Int 2008; 34(7):1747–51.

[9] Zhao YF, Ma Triblock co-polymer templating synthesis of mesostructured hydroxyapatite. J. Micro.and Meso. Mater.2005; 87:110-17.

[10] Zhang HB, Zhou K, Li Z, Huang S. Plate-likehydroxyapatite nanoparticles synthesized by the hydrothermal method. J. Phys. Chem. Solids 2009;70:243–248.

[11] Liu J, Ye X, Wang H, Zhu M, Wang B, Yan H. The influence of pH and temperature on the morphology of hydroxyapatite synthesized by hydrothermal method. Ceram. Int. 2003;29:629–633.

[12] Zhu A, Yan Lu, Yunfeng Si, Sheng Dai. Frabicating hydroxyapatite nanorods using a biomacromolecule template. Appl. Surf. Sci. 2011;257:3174–79.

[13] Zhang Y, Lu J. A simple method to tailor spherical nanocrystal hydroxyapatite at low temperature. *J. Nanopart. Res.* 2007;9:589-94.

[14] Cai Y, Pan H, Xu X, Hu Q, Li L, Tang R. Ultrasonic Controlled Morphology Transformation of Hollow Calcium Phosphate Nanospheres: A Smart and Biocompatible Drug Release System. *Chem. Mater* 2007;19:3081-83

[15] Shanthi PMSL, Mangalaraja RV, Uthirakumar AP, Velmathi S, Balasubramanian T, Ashok M. Synthesis and characterization of porous shell-like nano hydroxyapatite using Cetrimide as template. J.Colloid Interface. Sci 2010;350:39-43.

[16] Sasikumar S, Vijayaraghavan R.Solution combustion synthesis of bioceramic calcium phosphates by single and mixed fuels- A comparative study. Ceram. Int.2008;**34:**1373-79.

[17] Anee Kuriakose T, Narayana Kalkura S, Palanichamy M, Arivuoli D, Karsten D, Bocelli G et al. Synthesis of stoichiometric nano crystalline hydroxyapatite by ethanol-based sol–gel technique at low temperature. J. Cryst. Growth 2004;263:517-23.

[18] Anastasios A, Liarokapis E, Leventouri T. Micro-Raman and FT-IR studies of synthetic and natural apatites.Biomaterials2007;28:3043–54.

[19] Landi E, Tampieri A, Celotti G, Sprio S.Densification behaviour and mechanisms of synthetic Hydroxyapatites. *J. Eur.Ceram*. 2000; 20:2377-87.

[20] Elliott JC,Wilson RM, Dowker SEP.Apatite Stuctures. Adv. X-ray Anal. 2002;45: 172-81.

[21] Suryanarayana C, Grant Norton M.X-ray Diffraction-A Practical Approach. New York and London:Plenum Press; 1998.

[22] V. Biju, S. Neena, V. Vrinda, S.L. Salini, Estimation of lattice strain innanocrystalline silver from X-ray diffraction line broadening, J. Mater.Sci. 43 (2008) 1175–1179.

[23] Salarian M, Hashjin MS, Shafiei SS, Salarian R, Nemati ZA. Template-directed hydrothermal synthesis of dandelion-like hydroxyapatite in the presence of cetyltrimethylammonium bromide and polyethylene glycol.Ceram. Inter. 2009;35:2563-69.